Oil & Natural Gas Technology

DOE Award No.: DE-FC26-05NT42660

Quarterly Technical Progress Report

Analysis Of Critical Permeablity, Capillary Pressure And Electrical Properties For Mesaverde Tight Gas Sandstones From Western U.S. Basins

Submitted by:
University of Kansas Center for Research, Inc.
2385 Irving Hill Road
Lawrence, KS 66044

Prepared for:
United States Department of Energy
National Energy Technology Laboratory

September 30, 2007

Office of Fossil Energy

QUARTERLY TECHNICAL PROGRESS REPORT
FOR THE PERIOD ENDING SEPTEMBER 30, 2007

TITLE: ANALYSIS OF CRITICAL PERMEABLITY, CAPILLARY PRESSURE AND ELECTRICAL PROPERTIES FOR MESAVERDE TIGHT GAS SANDSTONES FROM WESTERN U.S. BASINS

DOE Contract No. DE-FC26-05NT42660

Contractor:	University of Kansas Center for Research, Inc. 2385 Irving Hill Road Lawrence, KS 66044
DOE Program:	Natural Gas Technologies (Advanced Diagnostics & Imaging)
Award Date:	October 1, 2005
Total Project Budget:	$513,834
DOE Cost Amount:	$411,030
Program Period:	October 1, 2005 – June 30, 2008
Reporting Period:	July 1, 2007 – September 30, 2007
DOE Project Manager:	Purna Halder, NETL Tulsa, OK
Contractor Contact:	Alan P. Byrnes Kansas Geological Survey 1930 Constant Ave., Lawrence, Kansas 66047 email: abyrnes@kgs.ku.edu phone: 785-864-2177
Principal Investigators:	Alan P. Byrnes (Program Manager) Robert Cluff (Discovery Group) John Webb (Discovery group)

DISCLAIMER:

ABSTRACT:

Wireline logs have been digitized, quality checked, core depth shifted to match log depth, and standard interpretation and analysis performed for all wells with complete log suite. Intrepreted logs have been posted to the project website: http://www.kgs.ku.edu/mesaverde/reports.html

Most of the critical gas saturation (S_{gc}) data support the commonly applied assumption that $S_{gc} < 0.05$. However, a few heterolithic samples exhibiting higher S_{gc} indicate the dependence of S_{gc} on pore network architecture and scale. Concepts from percolation theory and upscaling indicate that S_{gc} varies among four pore network architecture models: 1) percolation (N_p), 2) parallel ($N_{//}$), 3) series ($N_{\perp}$), and 4) discontinuous series ($N_{\perp d}$). Analysis suggests that S_{gc} is scale- and bedding-architecture dependent in cores and in the field.

The models suggest that S_{gc} is likely to be very low in cores with laminae and laminated reservoirs and low (e.g., $S_{gc} < 0.03$-0.07 at core scale and $S_{gc} < 0.02$ at reservoir scale) in massive-bedded sandstones of any permeability. In cross-bedded lithologies exhibiting series network properties, S_{gc} approaches a constant reflecting the capillary pressure property differences and relative pore volumes among the beds in series. For these networks S_{gc} can range widely but can reach high values (e.g., $S_{gc} < 0.6$). Discontinuous series networks, representing lithologies exhibiting series network properties but for which the restrictive beds are not sample-spanning, exhibit S_{gc} intermediate between N_p and $N_{\perp}$ networks.

Results for the project, to date, are being presented in a combined oral and poster presentation at the American Association of Petroleum Geologists Regional Annual Meeting in Snowbird, Utah, Oct. 9-10, 2997.

TABLE OF CONTENTS

LIST OF FIGURES

Acronyms

D	Fractal dimension
E	Euclidean dimension
f	Fraction of total network sites where gas nucleation occurs
k	Permeability, mD
k_{rg}	Relative permeability to gas, fractionl (v/v)
$k_{rg,Sw}$	Relative permeability to gas at a specific water saturation S_w, fraction (v/v)
L	Network size, number of nodes
N_p	Percolation network, random
$N_{//}$	Parallel network
$N_{\perp}$	Series network
$N_{\perp \mathrm{d}}$	Discontinuous series network
Pc	Capillary pressure, Pa
$Pc_{\mathrm{Sgc,high}}$	Capillary pressure at $S_{gc,high}$
ϕ	Porosity, fraction (v/v)
$S_{g,Pc\text{-}Sgc,high}$	Gas saturation at $Pc_{Sgc,high}$
S_{gc}	Critical gas saturation, expressed as a fractional (v/v) hydrocarbon saturation (1-S_w), saturation below which k_{rg} = 0
$S_{gc,\ low}$	Lowest critical gas saturation in parallel network, fraction (v/v)
$S_{gc,high}$	Highest critical gas saturation in series network, fraction (v/v)
S_w	Water saturation, fraction (v/v)
S_{wc}	Critical water saturation, fraction (v/v), saturation below which k_{rw} = 0
$S_{wc,g}$	Critical water saturation, fraction (v/v) with respect to gas drainage, saturation at which k_{rg} = 1 and below which k_{rg} = 1
V	System volume (v)

INTRODUCTION

Objectives - Industry assessment of the regional gas resource, projection of future gas supply, and exploration programs require an understanding of the reservoir properties and accurate tools for formation evaluation of drilled wells. The goal of this project is to provide petrophysical formation evaluation tools related to relative permeability, capillary pressure, electrical properties and algorithm tools for wireline log analysis. Major aspects of the proposed study involve a series of tasks to measure drainage critical gas saturation, capillary pressure, electrical properties and how these change with basic properties such as porosity, permeability, and lithofacies for tight gas sandstones of the Mesaverde Group from six major Tight Gas Sandstone basins (Washakie, Uinta, Piceance, Upper Greater Green River, Sand Wash and Wind River). Critical gas saturation (Sgc) and ambient and *in situ* capillary pressure (Pc) will be performed on 150 rocks selected to represent the range of lithofacies, porosity and permeability in the Mesaverde.

Project Task Overview -

Task 1. Research Management Plan
Task 2. Technology Status Assessment
Task 3. Acquire Data and Materials
    Subtask 3.1. Compile published advanced properties data
    Subtask 3.2. Compile representative lithofacies core and logs from major basins
    Subtask 3.3. Acquire logs from sample wells and digitize
Task 4. Measure Rock Properties
    Subtask 4.1. Measure basic properties (k, ϕ, grain density) and select advanced population
    Subtask 4.2. Measure critical gas saturation
    Subtask 4.3. Measure in situ and routine capillary pressure
    Subtask 4.4. Measure electrical properties
    Subtask 4.5. Measure geologic and petrologic properties
    Subtask 4.6. Perform standard logs analysis
Task 5. Build Database and Web-based Rock Catalog
    Subtask 5.1. Compile published and measured data into Oracle database
    Subtask 5.2. Modify existing web-based software to provide GUI data access
Task 6. Analyze Wireline-log Signature and Analysis Algorithms
    Subtask 6.1. Compare log and core properties
    Subtask 6.2. Evaluate results and determine log-analysis algorithm inputs
Task 7. Simulate Scale-dependence of Relative Permeability
    Subtask 7.1. Construct basic bedform architecture simulation models
    Subtask 7.2. Perform numerical simulation of flow for basic bedform architectures
Task 8. Technology Transfer, Reporting, and Project Management
    Subtask 8.1 Technology Transfer
    Subtask 8.2. Reporting Requirements
    Subtask 8.3. Project Management

EXECUTIVE SUMMARY:

Most of the S_{gc} data support the commonly applied assumption that $S_{gc} < 0.05$. However, a few heterolithic samples exhibiting higher S_{gc} indicate the dependence of S_{gc} on pore network architecture and scale. Concepts from percolation theory and upscaling indicate that S_{gc} varies among four pore network architecture models: 1) percolation (N_p), 2) parallel ($N_{//}$), 3) series ($N_{\perp}$), and 4) discontinuous series ($N_{\perp d}$). Analysis suggests that S_{gc} is scale- and bedding-architecture dependent in cores and in the field.

The models suggest that S_{gc} is likely to be very low in cores with laminae and laminated reservoirs and low (e.g., $S_{gc} < 0.03$-0.07 at core scale and $S_{gc} < 0.02$ at reservoir scale) in massive-bedded sandstones of any permeability. In cross-bedded lithologies exhibiting series network properties, S_{gc} approaches a constant reflecting the capillary pressure property differences and relative pore volumes among the beds in series. For these networks S_{gc} can range widely but can reach high values (e.g., $S_{gc} < 0.6$). Discontinuous series networks, representing lithologies exhibiting series network properties but for which the restrictive beds are not sample-spanning, exhibit S_{gc} intermediate between N_p and $N_{\perp}$ networks.

RESULTS AND DISCUSSION:

TASK 4. MEASURE ROCK PROPERTIES

Subtask 4.6. Perform standard logs analysis

Standard log analysis has been performed on all the primary wells. These analyses incorporate: wireline quality control, depth correction for core to log depth, calculation of porosity from density log response using matrix densities appropriate to basin, water saturations calculated using a standard Archie equation with constant cementation exponent. Figure 1 illustrates a portion of an example log interpretation available on the website.

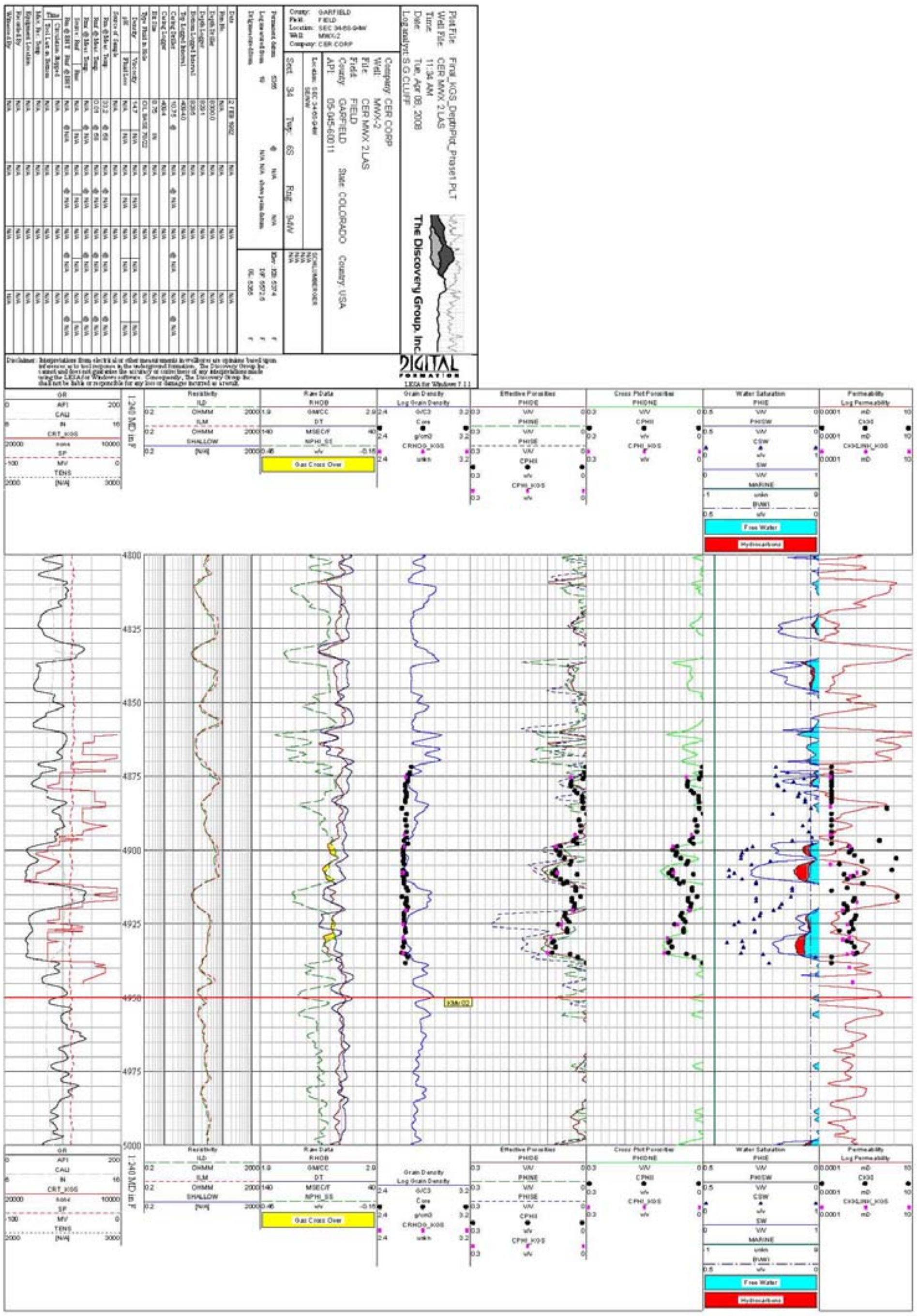

Figure 1. Example of wireline log presenting standard log analysis interpretation. Logs for other wells are available on the project website: http://www.kgs.ku.edu/mesaverde/reports.html

TASK 7. SIMULATE SCALE-DEPENDENCE OF RELATIVE PERMEABILITY

Subtask 7.1. Construct basic bedform architecture simulation models

Initial results of critical gas saturation (S_{gc}) measurements and interpretation were presented at the AAPG Hedberg Conference at Vail in 2005. This early research led to this study of critical gas saturation. The results of the earlier work and the results found to date in this study were combined and presented in a publication for the Hedberg Conference Proceedings that will be published by the AAPG in 2007. A more complete analysis of the critical gas saturation results is presented in the paper; Byrnes, A.P., (2007), Issues with gas and water relative permeability in low-permeability sandstones, Proceedings Am. Assoc. Petroleum Geologists, Hedberg Research Conference, "Understanding, Exploring and Developing Tight Gas Sands," April 24-29, 2005, Vail, Colorado, Chapter 5, p 1-14.

Most of the S_{gc} data support the commonly applied assumption that $S_{gc} < 0.05$. However, a few heterolithic samples exhibiting higher S_{gc} indicate the dependence of S_{gc} on pore network architecture and scale. Concepts from percolation theory and upscaling indicate that S_{gc} varies among four pore network architecture models: 1) percolation (N_p), 2) parallel ($N_{//}$), 3) series ($N_{\perp}$), and 4) discontinuous series ($N_{\perp \mathrm{d}}$). Analysis suggests that S_{gc} is scale- and bedding-architecture dependent in cores and in the field.

The models suggest that S_{gc} is likely to be very low in cores with laminae and laminated reservoirs and low (e.g., $S_{gc} < 0.03$-0.07 at core scale and $S_{gc} < 0.02$ at reservoir scale) in massive-bedded sandstones of any permeability. In cross-bedded lithologies exhibiting series network properties, S_{gc} approaches a constant reflecting the capillary pressure property differences and relative pore volumes among the beds in series. For these networks S_{gc} can range widely but can reach high values (e.g., $S_{gc} < 0.6$). Discontinuous series networks, representing lithologies exhibiting series network properties but for which the restrictive beds are not sample-spanning, exhibit S_{gc} intermediate between N_p and $N_{\perp}$ networks.

The physics and petroleum literature exploring percolation theory and application to porous media is extensive. Sahimi (1993, 1994) provides a comprehensive review. Berkowitz and Ewing (1998) review application to soils and Du and Yortsos (1999) summarize work on gas bubble growth and percolation. Beyond the experimental, critical-gas saturation work cited above, studies have investigated various aspects of two-phase percolation including issues with; mathematics of percolation in networks (Larson et al., 1977; Larson et al., 1981; Wall and Brown, 1981; Chandler et al., 1982; Koplik and Lasseter, 1982; Lenormand et al., 1983, 1985; Feder, 1988); invasion percolation (Wilkinsen and Willemsen, 1983), invasion under buoyant force (Wilkinson, 1984, 1986); invasion with trapping (Yanuka and Balberg, 1991); surface effects (Yortsos and Parlar, 1989; Cafiero et al., 1997); gas bubble formation, growth and percolation as a function of fraction of nucleation sites and capillary number (Li and Yortsos, 1995a, 1995b; Du and Yortsos, 1999; Ferer et al., 2003). Using a variety of methods Lin and Cohenm (1982), Koplik et al. (1984) and Yanuka et al. (1986) estimated that average coordination numbers, Z, for sandstones range between approximately 4 and 8, indicating that a simple cubic lattice with Z=6 is appropriate for representing rock pore network topology.

Gas invasion of a reservoir can be envisioned to be sufficiently slow that concentration profiles should be quasi-static similar to the stepwise increase associated with the measurement of a drainage capillary pressure curve. In this process, the invasion of gas into the water-saturated reservoir is represented by growth of a cluster(s) where gas–liquid interfaces in any gas-occupied pore advance one-at-a-time by invading perimeter pore throats in order of increasing capillary resistance (or corresponding decreasing radius). This process has been termed invasion percolation (Wilkinson and Willemsen, 1983; Feder, 1988) for invasion from one side or point on the perimeter of a network, and is a simpler form of invasion percolation where growth occurs from multiple clusters (Yortsos and Parler, 1989).

Wilkinson and Willemsen (1983) showed that the volume fraction of the percolation threshold, equivalent to S_{gc}, scales with network dimension, L, as:

$$S_{gc}(L) = A\, L^{D-E} \qquad (1)$$

where A is a numerical constant, D is the mass fractal dimension of the percolation cluster (D = 1.89 for 2-D, D = 2.52 for 3-D), E is the Euclidean dimension (E = 2 for 2-D and E = 3 for 3-D). For a simple 3-D cubic network A ≈ 0.65. This relation indicates that as $L \to \infty$ $S_{gc} \to 0$ (e.g., S_{gc} = 0.215 for L = 10; S_{gc} = 0.024 for L = 1,000; S_{gc} = 0.008 for L = 10,000).

Li and Yortsos (1993, 1995a) and Du and Yortsos (1999) extended the invasion percolation work to include gas nucleation at one or more sites showing that S_{gc} scales with network size, L, and the fraction of total network sites where gas nucleation occurs, f, as:

$$S_{gc}(L; fq) = A\, L^{D-E} + B\, f^{\,1-D/E} \qquad (2)$$

where A and B are numerical constants, D is the mass fractal dimension of the percolation cluster (D = 1.89 for 2-D OP, D = 1.82 for 2-D IP with trapping, D = 2.52 for 3-D OP or IP, with or without trapping), E is the Euclidean dimension (E = 2 for 2-D and E = 3 for 3-D), and f is the fraction of total network sites where gas nucleation occurs. In the limit of very small f (e.g., one nucleation site only or external drive) the second term is approximately zero and S_{gc} corresponds to the volume fraction of the percolation cluster only, as presented in Equation 1. When the nucleation fraction increases, the main contribution to S_{gc} results from clusters growing around nucleation sites and not from the percolation cluster (Du and Yortsos, 1999). For large networks the first term in Equation 2 vanishes and S_{gc} becomes primarily a function of the fraction of nucleation sites.

Pore Networks and k_{rg}, S_{gc}

Pore networks can be broadly classified as exhibiting three end-member architectures and an important intermediate architecture: 1) Percolation network (N_p)- random orientation of pore sizes within the network, 2) Parallel network ($N_{//}$)- preferential orientation of pore sizes or beds of different N_p networks parallel to the invasion direction, 3) Series network ($N_\perp$) - preferential sample-spanning orientation of pore sizes or beds of different N_p networks perpendicular to the invasion direction, and 4) Discontinuous series network ($N_{\perp d}$) - preferential non-sample-spanning orientation of pore sizes or beds of different N_p networks perpendicular to the invasion direction (Figure 2). Different sandstone lithologies and the four pore-networks and their relationship to S_{gc} and k_{rg} is discussed. Gas is used as the invading phase for the following discussion.

Percolation Network (N_p)

A massive-bedded or uniformly bioturbated sandstone, siltstone, or shale might exhibit a pore network that can be represented by a percolation network. As discussed above, for this network, formation of the percolation cluster would occur at S_g < 0.03-0.07 at the core-plug scale and would approach S_{gc} < 0.01-0.02 at large scales following Equation 1. Massive-bedded sandstone and siltstone is a common lithology in low-permeability sandstones and therefore low S_{gc} is likely to be common in many reservoir systems.

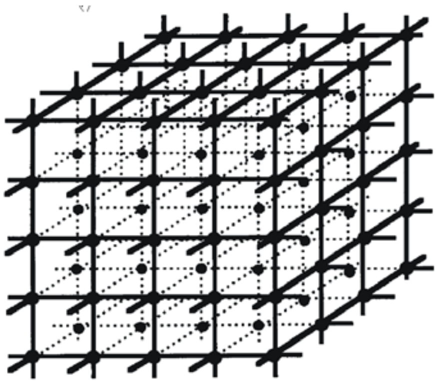

1) Percolation Network (N_p) - Macroscopically homogeneous, random distribution of bond sizes, e.g., Simple Cubic Network (z=6)

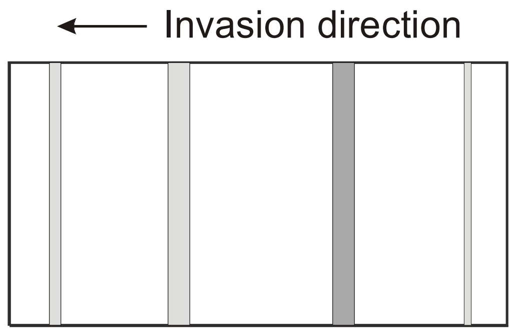

3) Series network ($N_\perp$) - preferential sample-spanning orientation of pore sizes or beds of different N_p networks perpendicular to the invasion direction.

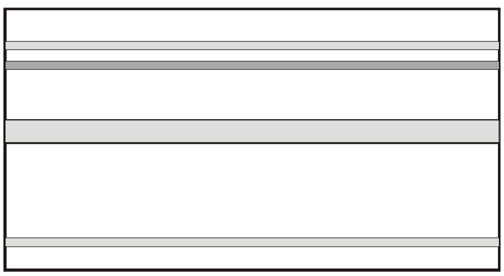

2) Parallel Network ($N_{\parallel}$) preferential orientation of pore sizes or beds of different N_p networks parallel to the invasion direction.

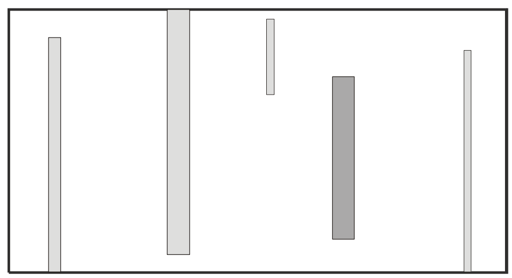

4) Discontinuous series network ($N_{\perp d}$) - preferential non-sample-spanning orientation of pore sizes or beds of different *Np* networks perpendicular to the invasion direction. Represents continuum between N and N_p.

Figure 2. Conceptual pore network models: 1) percolation (N_p), 2) parallel ($N_{//}$), 3) series ($N_\perp$), and 4) discontinuous series ($N_{\perp d}$).

Parallel Network ($N_{//}$)

Planar- and horizontally-laminated bedding is common in marine and tidal flat environments. In addition, many sedimentary structures that might be Series Networks on a large scale can exhibit $N_{//}$ properties at smaller scales including core scale. Parallel networks perform similarly to percolation networks except that portions of the network are not involved in the invasive flow associated with establishing S_{gc}. The critical-gas saturation of this system is the critical saturation of the lowest threshold-entry pressure layer ($S_{gc,low}$; generally the highest-permeability layer) within the system, volumetrically normalized to the total system volume to express the critical saturation relative to the total system volume (S_{gc}). Because the volume of the layer is less than the volume of the total system, the network dimension is smaller and $S_{gc,low}$, from Equation 1, is greater than if the entire system exhibited the percolating layer properties. However, renormalization of the layer $S_{gc,low}$ to the total system volume results in a lower S_{gc}. Since S_{gc} approaches $S_{gc} < 0.02$ at large scales in percolating systems, it approaches similar or lower values in parallel systems. It is important to note that many rocks exhibit microscopic to millimeter-scale lamination. The presence of a single, sample-spanning, one-millimeter-thick lamina in a core, even with high $S_{gc,low}$, can result in a very low S_{gc} value for the core (e.g., a lamina with $S_{gc,low} = 0.5$, representing 1% of the total core volume, results in a core $S_{gc} = 0.005$). Frequently, core sampling procedures avoid sampling series flow architecture by orienting plugs parallel to bedding, thereby creating a sample with $N_{//}$ properties. Following establishment of S_{gc}, the total system gas relative permeability represents the vector solution of the various layer relative permeabilities both parallel to flow and between layers (cross-flow).

Series Network ($N_{\perp}$)

Sedimentary bedding structures that represent series networks in one or more dimensions at one or more scales are abundant in nature (e.g., trough cross-bedding, large- and small-scale planar cross-bedding, low-angle planar bedding, hummocky bedding, Flaser bedding). Within these structures scales of series networks range from millimeter-scale laminae to decameter scale cross-bedding. If the continuity of the beds is broken such that the beds are not sample-spanning then the series network is discontinuous as discussed below.

In a $N_{\perp}$ network, percolation across the system does not occur until the invading gas pressure equals or exceeds the threshold pressure ($Pc_{Sgc,high}$) required to achieve critical saturation in the single barrier-bed with the highest pressure needed to allow percolation through that barrier-bed ($S_{gc,high}$). If invasion occurs under equilibrium-capillary pressure conditions then S_{gc} for the entire system is a function of the capillary-pressure properties of the barrier-beds in the system and is the average of the individual bed saturations at $Pc_{Sgc,high}$ ($S_{g,Pc\text{-}Sgc,high}$) normalized for bed pore volumes :

$$S_{gc} = [\Sigma(S_{g,Pc\text{-}Sgc,high})_i \phi_i V_i] \,/\, [\Sigma \phi_i V_i] \tag{3}$$

Figure 3 illustrates a simple cross-bedded system consisting of two lithologies that exhibits very high S_{gc} as a result of the significant difference in the capillary pressure properties of the beds (e.g., siltstone laminae within sandstone). Corey and Rathjens (1956) observed critical-gas saturations of 0.60 in a cross-bedded sandstone with flow perpendicular to bedding.

$S_{gc,high}$ for the most-restrictive barrier-bed can be considered to follow Equation 1 and approaches zero at infinite size. However, the system S_{gc} does not approach zero but approaches a constant since the adjacent beds are all at the saturations associated with the threshold pressure of the restrictive barrier-bed. Equilibrium capillary-pressure conditions result in the maximum S_{gc} for a system. For systems with a pressure gradient across the system (e.g., flowing core test) S_{gc} is reduced as a result of the lower capillary pressures, and consequent lower gas saturations, in the down-gradient portion of the system. Given the time frames available, reservoirs are likely to be charged under capillary pressure equilibrium conditions.

Average absolute permeability in series flow has been shown to be the harmonic average of the bed permeabilities. Weber (1982) presented equations for calculating directional permeability in common cross-bedding structures. Directional, gas-relative permeability can be calculated using similar methodology. It is important to note that most reservoir-, flow-simulation software treat capillary pressure and relative permeability as scalars and do not provide directional components (e.g., krg_x, krg_y, Pc_x, etc.) as they do for permeability (e.g., k_x, k_y, k_z)

Discontinuous Series Network ($N_{\perp d}$)

The $N_{\perp}$ network discussed above requires that the barrier-beds be sample-spanning perpendicular to the direction of invasion. Beds may not be sample-spanning or may have holes. These represent discontinuous series networks ($N_{\perp d}$) and represent a continuum between a

Percolation, N_p, and a Series, $N_\perp$, network. Critical saturations in a $N_{\perp d}$ network range between N_p and $N_\perp$ critical saturations as a function of the network size, and the frequency, length, and property differences among the discontinuous barriers and the "host" sample-spanning network. Fundamentally, since a continuous path across the system exists through the "host" network, S_{gc} in a $N_{\perp d}$ network follows Equation 1. However, because some potential paths for the sample-spanning cluster are blocked, at any given network dimension, more "pretender" paths (Thompson et al., 1987) are formed and S_{gc} is greater than for a N_p network of the same dimension. Though a formal mathematical analysis is not known, it can be estimated that S_{gc} in a $N_{\perp d}$ network follows Equation 1 but exhibits a decrease in slope as barrier-beds approach sample-spanning dimensions.

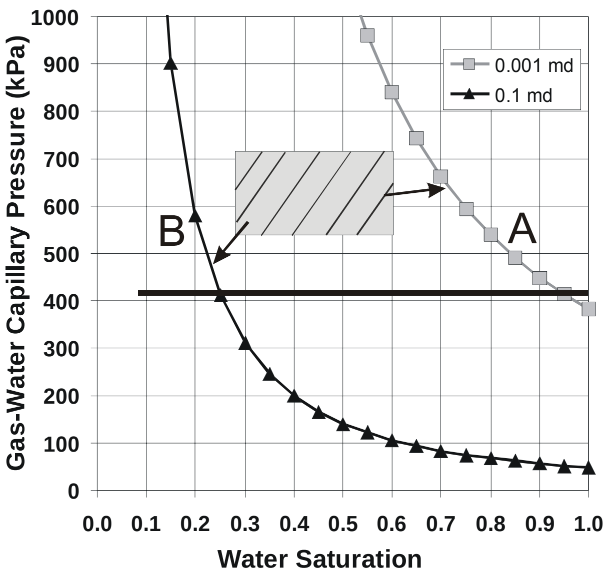

Figure 3. Example for a cross-bedded sandstone, consisting of higher-permeability/low- capillary-pressure sandstone (B) interbedded with low-permeability/high-capillary-pressure siltstone laminae (A), showing how S_{gc} can reach high values for invasion in a series network. For gas to flow across this system it must exceed the capillary pressure for the S_{gc} of the 0.001 mD fine beds ($Pc_{Sgc,high}$ on curve A). At $Pc_{Sgc,high}$ the 0.1 mD sandstone is desaturated to $S_{g,Pc\text{-}Sgc,high}$ = 0.75. Assuming that the pore volume of the shale is negligible, the volume of this rock is largely the 0.1 mD facies and S_{gc} =0.75.

TASK 8. TECHNOLOGY TRANSFER, REPORTING, PROJECT MANAGEMENT

Subtask 8.1 Technology Transfer

A combined oral and poster presentation is being presented at the Rocky Mountain Section meeting of the American Association of Petroleum Geologists at Snowbird, UT in October 6-9, 2007. The presentations will present results of Mesaverde properties measured. The talk and poster are being posted on the website.

Subtask 8.3. Project Management

In August a no-cost extension for the Project was submitted requesting extension to June 30, 2008. This extension was granted.

CONCLUSIONS

Wireline logs have been digitized, quality checked, core depth shifted to match log depth, and standard interpretation and analysis performed for all wells with complete log suite. Intrepreted logs have been posted to the project website: http://www.kgs.ku.edu/mesaverde/reports.html. Advanced log analysis is proceeding.

Most of the critical gas saturation (S_{gc}) data support the commonly applied assumption that $S_{gc} < 0.05$. However, a few heterolithic samples exhibiting higher S_{gc} indicate the dependence of S_{gc} on pore network architecture and scale. Concepts from percolation theory and upscaling indicate that S_{gc} varies among four pore network architecture models: 1) percolation (N_p), 2) parallel ($N_{//}$), 3) series ($N_{\perp}$), and 4) discontinuous series ($N_{\perp d}$). Analysis suggests that S_{gc} is scale- and bedding-architecture dependent in cores and in the field.

Results for the project, to date, are being presented in a combined oral and poster presentation at the American Association of Petroleum Geologists Regional Annual Meeting in Snowbird, Utah, Oct. 9-10, 2997. A no-cost extension to June 30, 2008 was requested and granted.

REFERENCES

Key references only

Broadbent, S.R., and J.M. Hammersley, 1957, Percolation processes I. Crystals and mazes, Proceedings of the Cambridge Philosophical Society, v. 53, p. 629-641.

Du, C., and Y.C. Yortsos, 1999, A numerical study of the critical gas saturation in a porous medium, Transport in Porous Media, v. 35, p**.** 205–225.

Li, X. and Y.C. Yortsos, 1993, Critical gas saturation: modeling and sensitivity studies, paper SPE 26662, Proceedings of the 68th Annual Technical Conference of the Soc. Petroleum Engineers, Houston, Texas, Oct. 3-6, p. 589-604.

Sahimi, M., 1994, *Applications of Percolation Theory*, Taylor and Francis, London, 258 pgs.

Thompson, A.H., A.J. Katz, and R.A. Raschke, 1987, Mercury injection in porous media: a resistance Devil's staircase with percolation geometry, Physical Review Letters, v. 58, no. 1, p. 29-32.

Wilkinson, D., 1984, Percolation model of immiscible displacement in the presence of buoyancy forces, Phys. Rev. A, v. 30, p. 520-531.

Wilkinson, D.: 1986, Percolation effects in immiscible displacement, Physical Review A, v. 34, p. 1380–1391.

Wilkinson, D., and J.F. Willemsen, 1983, Invasion percolation: a new form of percolation theory, J. Phys. Rev. A 16, p. 3365–3376.

Yanuka, M., and I. Balberg, 1991, Invasion percolation in a continuum model, J. Phys. **A:** Math. Gen., v. 24, p. 2565-2568.

Yortsos, Y. C. and M. Parlar, 1989, Phase change in binary systems in porous media: Application to solution gas drive, paper SPE 19697, Presented at the 1989 Society of Petroleum Engineers Fall Meeting, San Antonio, Texas, Oct. 8–9.

National Energy Technology Laboratory

626 Cochrans Mill Road
P.O. Box 10940
Pittsburgh, PA 15236-0940

3610 Collins Ferry Road
P.O. Box 880
Morgantown, WV 26507-0880

One West Third Street, Suite 1400
Tulsa, OK 74103-3519

1450 Queen Avenue SW
Albany, OR 97321-2198

2175 University Ave. South
Suite 201
Fairbanks, AK 99709

Visit the NETL website at:
www.netl.doe.gov

Customer Service:
1-800-553-7681